

Non-stationary high velocity jet impingement on small cylindrical obstacles

Prof.Dr. Miroslaw Weclas

Institut für Fahrzeugtechnik (IFZN)
Fakultät Maschinenbau u. Versorgungstechnik
Georg-Simon-Ohm-Hochschule für angewandte
Wissenschaften – Fachhochschule Nürnberg

Keßlerplatz 12
90489 Nürnberg

Abstract

Basic aspects of a high velocity Diesel jet interaction with small cylindrical obstacles are presented in the paper. The phenomenon discussed in the paper lies between cylinder overflow and jet impingement on to solid wall. Especially the effect of high velocity Diesel jet “destruction” and its distribution in space are investigated in the paper. As shown, the dominant role in this process plays a fist obstacle: its diameter, distance from the nozzle outlet and injection pressure play a dominant role in characterization of the jet distribution in space. The jet spatial distribution bases on a multi-jet model.

By Diesel jet impingement on a single obstacle with smaller diameter the distribution angle decreases with increasing injection pressure. For bigger obstacle the angle separating both jets increases being almost independent of the injection pressure. This angle does not change with time after impingement process, however decreases with increasing distance between nozzle and the obstacle.

For Diesel jet impingement on more than single obstacle, the jet distribution depends on the obstacle geometrical configuration but not necessarily on the number of obstacles. As shown in the paper quite similar distribution has been obtained for three and eight obstacles configurations. Presented phenomenological model explains this observation. There is possible to design such configuration of small obstacles which permit very good charge homogenization in defined space (combustion chamber).

1. Introduction

One of possible strategies for Diesel mixture homogenization and de-coupling of combustion from injection process would be late injection mode, what requires very quick spatial distribution of the Diesel jet and its homogenization in space. This could be promoted by injection in a porous medium [8]. It was observed that due to jet impingement on a large number of pore junctions of a highly porous 3D-structure, the Diesel jet may very quickly be distributed in space across the impingement direction. From one impinging jet a number of secondary jet are forming according to a multi-jet splitting effect described in [8,9]. The Diesel jet interaction with such three dimensional highly porous structure (see chapter 2 of the paper) may be simplified by Diesel jet impingement on small cylindrical obstacles giving similar effect for jet momentum distribution in space. This effect will be presented in this paper.

High velocity jet impingement on a small cylinder must be separated from the cylinder overflow, where depending on the Reynolds number the stream lines follow the cylindrical shape of the obstacles to flow separation and Karman vortex street behind the cylinder at higher Reynolds numbers. The goal of in the present paper investigated jet impingement on a small cylinder is to “destroy” the high velocity jet momentum and to distribute the mass in space. The process must also be different from the jet impingement on the solid wall where the axial jet propagation is quite blocked and only the radial flow along the wall is possible [1-7]. So, the phenomenon discussed in the present paper lies between cylinder overflow and jet impingement on to solid wall. This is the reason that, according to the author knowledge, there are no data available in the literature which describe investigated case, except similarity to Diesel jet impingement on to porous structure, as already described by the author in [8-10]. Thus, the goal of this paper is to describe the basic features and physics of a non-stationary high velocity jet impingement on small cylindrical obstacles for further application to mixture formation in Diesel engines.

The test rig and measurement technique used in present investigation are described in section 2, indicating two different experimental conditions used in the form of surrounding fluid: air and oil. Different geometrical configurations characterized by number of obstacles and their localization with respect to the Diesel nozzle are also described in this section. The section 3 presents data for Diesel jet impingement on a single cylindrical obstacle, for different injection pressures (impingement velocities), cylinder diameter and distance from the nozzle outlet.

The next chapter (section 4) describes the Diesel jet impingement on a number of obstacles: from 3 to 8 obstacles, depending on the investigated configuration. These results clearly indicate that the jet impingement on the first obstacle is a very critical factor for Diesel interaction with a number of small cylinders. Additionally, a geometrical configuration described by a relative location of obstacles defines the impingement result. On the basis of performed experimental investigations, a phenomenological model of Diesel jet impingement on a series of obstacles is presented in section 5 indicating the mechanism of jet distribution in space. This section also compares data of jet impingement obtained in air and oil. Results are then summarized in section 6.

2. Test rig and measurement technique

In order to perform a basic investigation on Diesel jet impingement on small obstacles a special test chamber has been used having very good optical access. The chamber has been built as a low pressure system (1bar at ambient temperature), with two different surrounding fluids to be applied: air and oil (Fig.1).

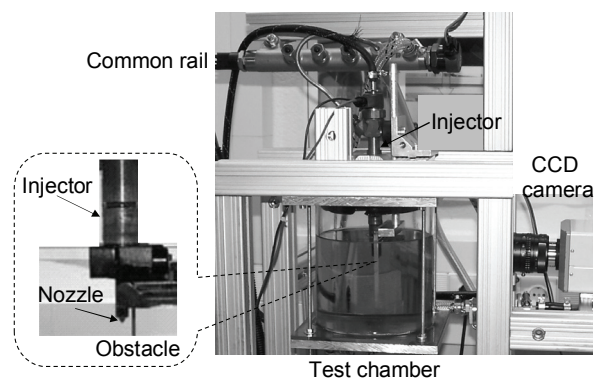


Figure 1: View of the test chamber with a Common-rail Diesel injection system

Diesel injection in oil bath (as a surrounding medium) has some additional features, very important for investigations of wall jet impingement. Firstly, no atomization may be observed during free jet formation and its propagation throughout the chamber volume (single phase system).

Secondly, the fuel vaporization process in oil bath is practically eliminated, and for applied temperatures (approx. 20 to 25°C) is negligible. For high time resolved investigations, a black-white CCD camera (PCO) model FlashCam has been used. The camera can externally be triggered (synchronized with

injection timing) with illumination time from 1 to 1000 μ s; additionally, the signal phase may be shifted with respect to the trigger signal in the range from 1 to 1000 μ s. For reported investigations a constant illumination time of 100 μ s has been applied.

Experimental configuration for Diesel jet impingement on a single or selected number of small cylindrical obstacles used in the present investigation is shown in Fig.2.

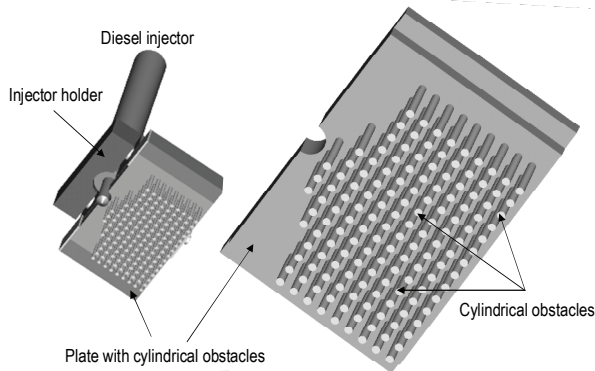


Figure 2: Experimental configuration for investigation of Diesel impingement on small cylindrical obstacles

There are number of different experimental configurations defined by a number of obstacles mounted on the plate as well as a position of individual obstacles. Distance between obstacles is twice of the obstacle diameter. The most important investigated geometrical configurations are detailed described in Fig.3.

Besides already defined geometrical configurations, the following measurement conditions have been used in the present investigation:

- Surrounding fluid: air and oil (most of experiments have been performed in oil)
- Injection pressure: 400bar, 800bar and 1200bar (for some experiments other pressure have also been used)
- Constant injection duration: 1500 μ s (for some experiments 3000 μ s has been used)
- Variable time after injection trigger signal: from 0 to 5000 μ s
- Variable time after impinging on the first obstacle: from 0 to 5000 μ s
- Three different view angles: bottom, side and back-view angles

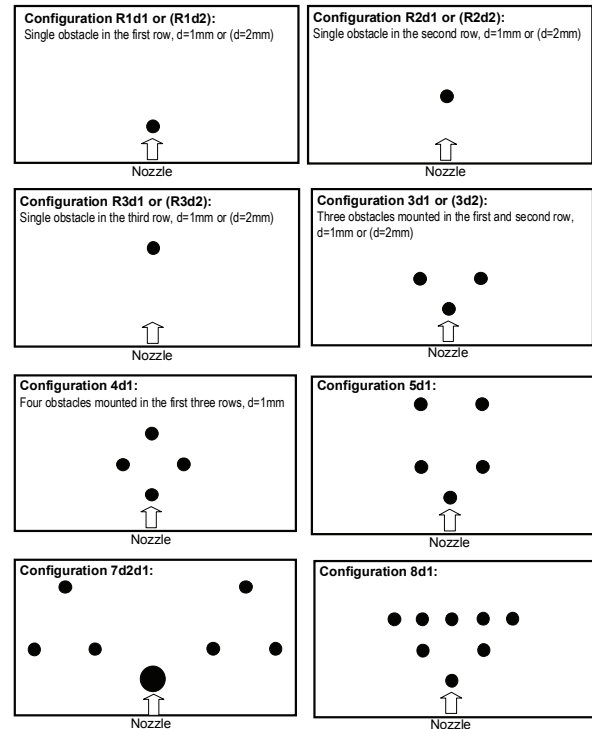


Figure 3: Specification of all investigated geometrical configurations

For the present investigations a special two-hole nozzle has been used, as already described in [8]. Fuel is injected horizontally into two opposite directions with a spray angle of 16° in air under atmospheric conditions.

3. Diesel jet impingement on a single cylindrical obstacle

As an initial investigation, a Diesel jet impingement on a single cylindrical obstacle is considered to recognize main parameters defining the jet distribution in space. It must be noticed, that in the present work the jet impingement on the cylinder but not cylinder overflow are investigated. If the distance between nozzle outlet and cylindrical obstacle is too large, i.e. the impingement velocity is relatively low, there is no impingement observed instead of cylinder overflow. Such data are shown in Table 1 and in Fig.4.

Table 1: Conditions for cylinder "over flow"

Parameter	Investigated configuration			
	(row number)			
Distance from the nozzle outlet [mm]	11 (row 4)	13 (row 5)	15 (row 6)	17 (row 7)
Free jet velocity in oil [m/s]	63.6	57.8	52.9	47.7
Diameter of cylindrical obstacle [mm]	1	1	1	1
Reynolds number	19569	17785	16277	14677

The diameter of the obstacle is small comparing to the jet front surface area preventing from solid-wall like impingement process [7,8].

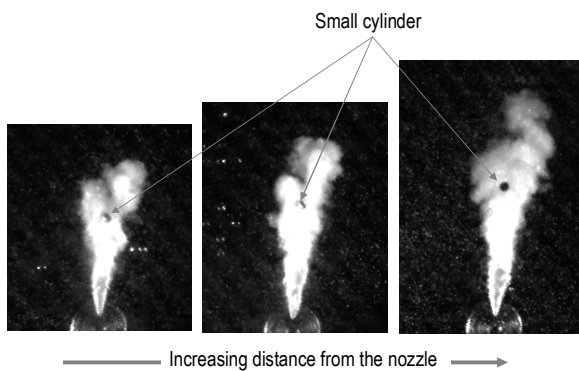


Figure 4: Cylinder overflow instead of jet impingement

In the first step configuration R1d1 is investigated as shown in Fig.5. This figure shows Diesel jet impingement on a single obstacle as a function of time after jet impingement for injection pressure 400bar. The effect of Diesel jet interaction with a small obstacle in the form of two jets may clearly be observed after impingement process. The distribution angle between both jets is shown in Table 2.

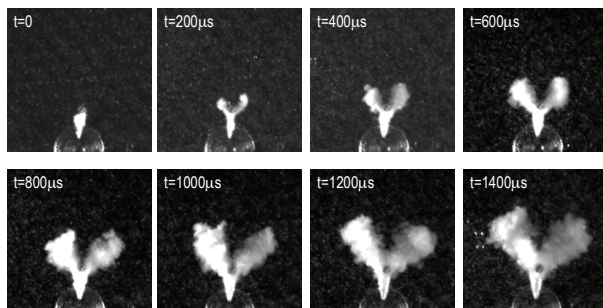
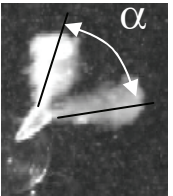


Figure 5: Diesel jet impingement on a single cylindrical obstacle (configuration R1d1) as a function of time after impingement for injection pressure 400bar

For smaller obstacle the distribution angle decreases with increasing injection pressure. For bigger obstacle (d=2mm) the angle separating both jets increases being almost independent of the injection pressure.

Table 2: Distribution angle by Diesel jet impingement on a single cylindrical obstacle

Configuration	Distribution angle	
	$\alpha [^\circ]$	
R1d1 at 400bar	93.2	
R1d1 at 800bar	70.8	
R1d1 at 1200bar	61.8	
R1d2 at 400bar	121.4	
R1d2 at 800bar	121.6	
R1d2 at 1200bar	118	

This angle does not change with time after impingement as indicated in Figure 6. The angle α however decreases with increasing distance between nozzle and the obstacle. At large distances from the nozzle outlet the angle α is still higher for bigger obstacle as for smaller one. Picture presented in Figure 5 and 6 shows the jets at the bottom view angle.

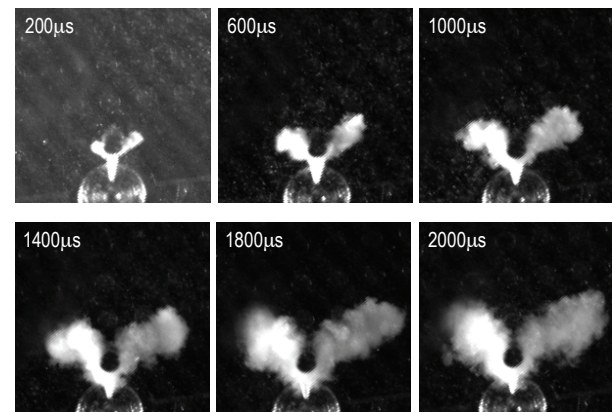


Figure 6: Diesel jet impingement on a single cylindrical obstacle (configuration R1d2) as a function of time after impingement for injection pressure 400bar

An influence of the distance between nozzle outlet and the obstacle is shown in Figure 7, where Diesel jet impingement on a single obstacle is investigated for configurations R1d1 and R2d1at 1000µs after impingement and for 800bar injection pressure.

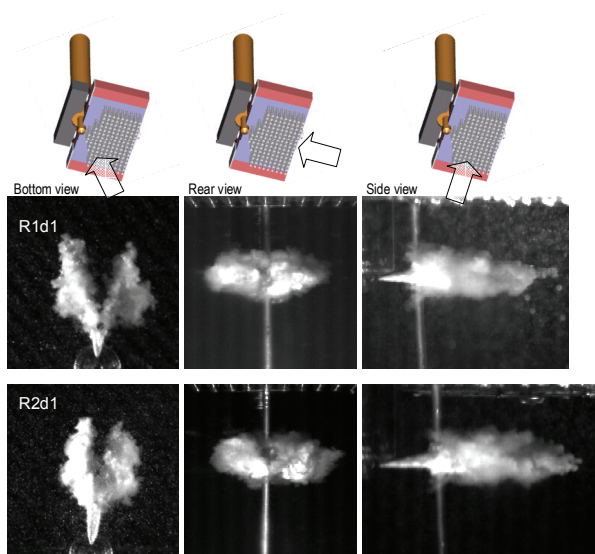


Figure 7: Diesel jet impingement on a single obstacle for two different distances between cylinder and nozzle outlet (configurations R1d1 and R2d1) at 1000µs after impingement and for 800bar injection pressure.

There are number of different parameters characterizing Diesel jet impingement process on a cylindrical obstacle. First of all the parameters in a bottom view angle may be defined, as shown in Figure 8a: jet length, jet width and jet surface area. Additionally, in the side view angle, jet height is defined as shown in Fig.8b.

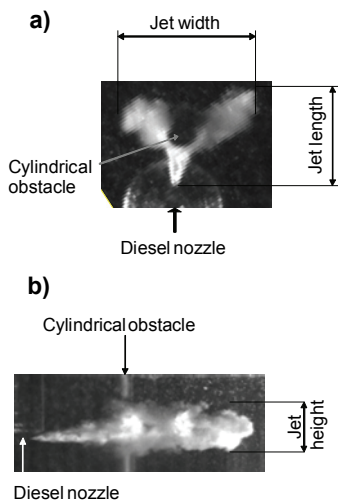


Figure 8: Definition of parameters characterizing jet impingement on a cylindrical obstacle for two view angles: a- bottom view, b-side view.

The length of the jets is quantified for investigated configurations and injection pressures in Figure 9. The jet length increases with increasing injection pressure, and is generally higher for smaller obstacle (d=1mm). Additionally, data for a free jet are also included in the picture.

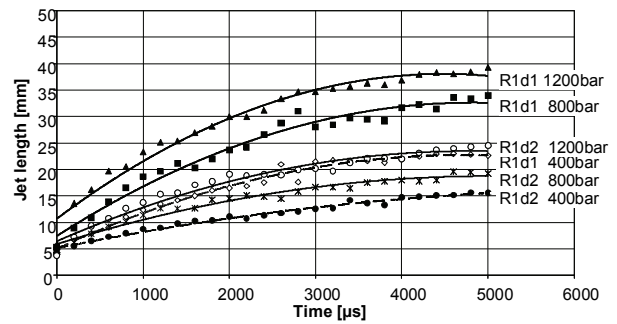


Figure 9: Jet length after impingement on a single cylindrical obstacle as a function of time for three different injection pressures and different surrounding fluids (configuration R1d1 and R1d2)

The next parameter characterizing the effect of jet impingement on the obstacle is the jet width, shown in Fig.10. The bigger the obstacle and the higher the injection pressure the wider distribution of impingement jet in space (jet width).

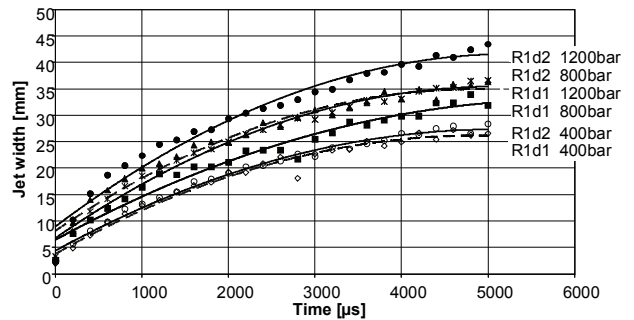


Figure 10: Jet width after impingement on a single cylindrical obstacle as a function of time for three different injection pressures and different surrounding fluids (configuration R1d1 and R1d2)

However the effect of the obstacle diameter on the jet distribution is weaker as it was observed for jet length. Both figures indicate, that in order to get short and wide jets a bigger cylindrical obstacle should be used for impinging Diesel jet. The final parameter characterizing Diesel jet impingement on a small obstacle from the bottom view angle is the jet surface area (Fig.11). In this case, the jet surface area measured from the bottom angle is bigger for smaller obstacle and increases with increasing injection pressure.

Above presented data for Diesel jet impingement on a single obstacle have been analysed from the bottom view angle. At the side view angle the jet impingement looks different, as shown in Fig.12. There are three injection pressures investigated in this figure for configuration R1d1 (left) and R2d2 (right) at time of 800µs after impingement on the cylindrical obstacle. Bigger obstacle makes jet distribution across the impingement direction bigger (side view angle).

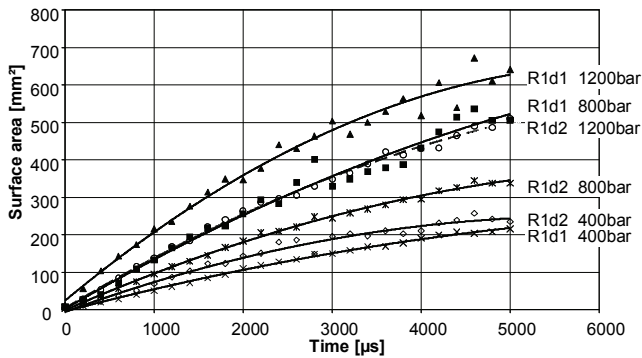


Figure 11: Jet surface area after impingement on a single cylindrical obstacle as a function of time for three different injection pressures and different surrounding fluids (configuration R1d1 and R1d2) (bottom view)

This pictures show also, that the impingement momentum is so large that the long cylindrical obstacle (especially with $d=1\text{mm}$) may significantly bend. The holding of this obstacle should be change to get a stable and stiff geometry.

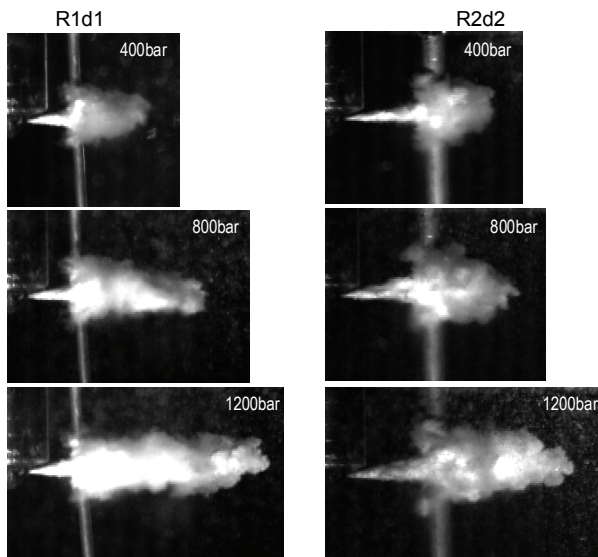


Figure 12: View of the jet impingement on a single cylindrical obstacle at a side view angle for three injection pressures, both investigated obstacle diameters at $t=800\mu\text{s}$ after jet impingement

The effect of jet impingement on a single obstacle from the side view angle may be characterized by the jet height as shown in Fig.13. As shown, the effect of the injection pressure on the jet height is clear for smaller obstacle, only. The jet height is bigger for bigger obstacle ($d=2\text{mm}$) and increases with time until reaching the maximal value. The last parameter to be used for characterizing of jet impingement on a single obstacle is the jet surface area at the side view angle (Fig.14). This jet surface area increases with injection pressure and with obstacle diameter.

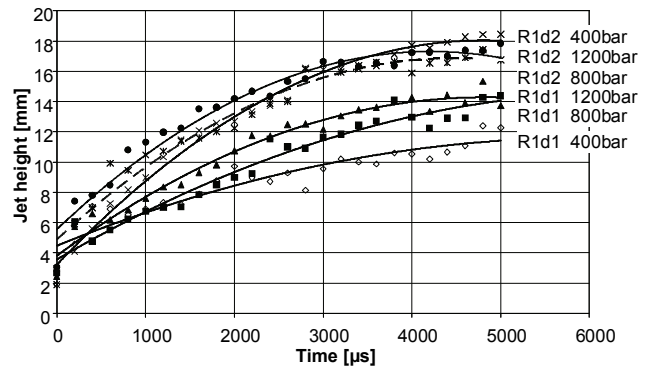


Figure 13: Jet height after impingement on a single cylindrical obstacle as a function of time for three different injection pressures and different surrounding fluids (configuration R1d1 and R1d2)

The data presented in above figures were obtained for configuration R1, i.e. the obstacle was mounted in the first row in the holding plate (see also Fig.6). It has been found for geometrical configurations R2 and R3 that with increasing distance between nozzle outlet and obstacle the length of the jet increases and the jet width decreases.

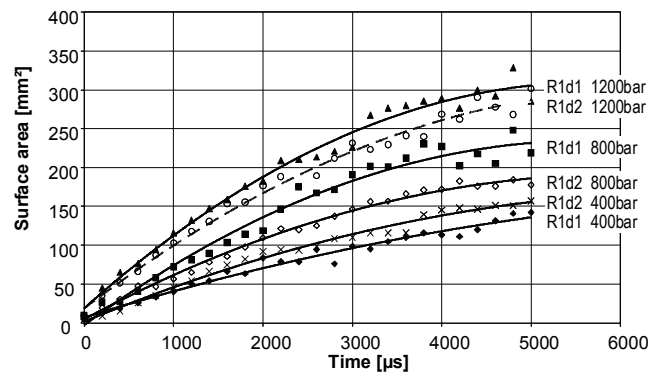


Figure 14: Jet surface area after impingement on a single cylindrical obstacle as a function of time for three different injection pressures and different surrounding fluids (configuration R1d1 and R1d2) (side view)

Also the jet surface area reduces with increasing distance from the nozzle. Additionally, with increasing distance from the nozzle the effect of the obstacle diameter is significantly reduced.

4. Diesel jet impingement on multiple-cylindrical obstacles

The next geometrical configuration to be investigated in this paper is characterized by three obstacles (configurations 3d1 and 3d2). General overview of the jet impingement on three cylindrical obstacles is given in figure 15 for three investigated injection pressures at different times after impingement on the first obstacle (R1d1).

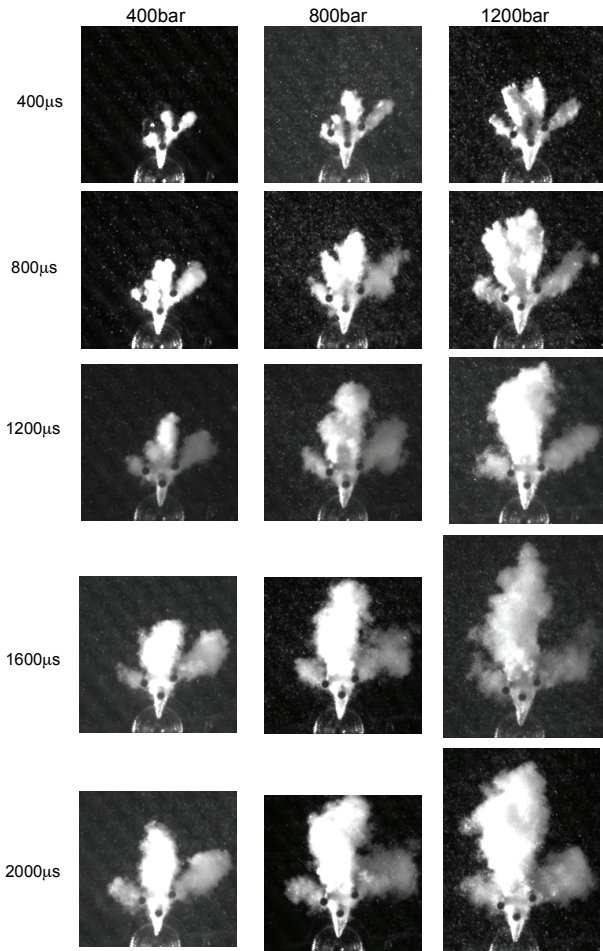


Figure 15: Jet impingement on three cylindrical obstacles for three different injection pressures at different times after impingement on the first obstacle (R1d1)

Obviously a third secondary jet after impingement on the first obstacle may be observed. This third jet is not clearly present in the case of bigger obstacle (Fig.16).

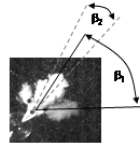


Figure 16: Jet impingement on three cylindrical obstacles for three different injection pressures and $d=2\text{mm}$ at $1600\mu\text{s}$ after impingement on the first obstacle

This figure shows Diesel jet impingement on three cylindrical obstacles of diameter $d=2\text{mm}$ for three investigated injection pressures at $1600\mu\text{s}$ after jet impingement on the first obstacle. This is a result of geometrical configuration to be investigated. Impingement on a single obstacle for $d=2\text{mm}$ indicated the angle α on the order of 120 degree mak-

ing impingement on two additional obstacles mounted in the second row unimportant. The distribution angles for three obstacles are defined and summarized in Table 3.

Table 3: Distribution angles by impingement on three obstacles (configuration 3d1)

Configuration		Angle β_1 [°]	Angle β_2 [°]
3d1, 400 bar, $t = 1400 \mu\text{s}$		51	20,8
3d1, 800 bar, $t = 1200 \mu\text{s}$		51,4	23
3d1, 1200 bar, $t = 800 \mu\text{s}$		59,6	25,8

5. Phenomenological model of Diesel jet impingement on small cylindrical obstacles

A three jets observed for configuration 3d1 indicated necessity of putting an additional obstacle on the way of the middle jet to get a good distribution in space (configuration 4d1). This effect is indicated in Figure 17 (left) presenting jet impingement in configuration of four obstacles. The first insight in the impingement process indicates similarity to the already analysed jet impingement on three obstacles.

The middle jet will clearly divided in to two jet giving together four singular jets to be recognized in the system. For more information on the role of obstacles mounted in rows 2 and 3, the system of 4-obstacles is modified to the eight small cylinders (8d1). This configuration consists of configuration 4d1 plus four additional obstacles in the row 3. Results of Diesel jet impingement on eight small obstacles is shown in Fig 17 (right) indicating quite similar impingement process to the configuration with 4-obstacles.

This “unexpected” similarity is clarified in Figure 18.

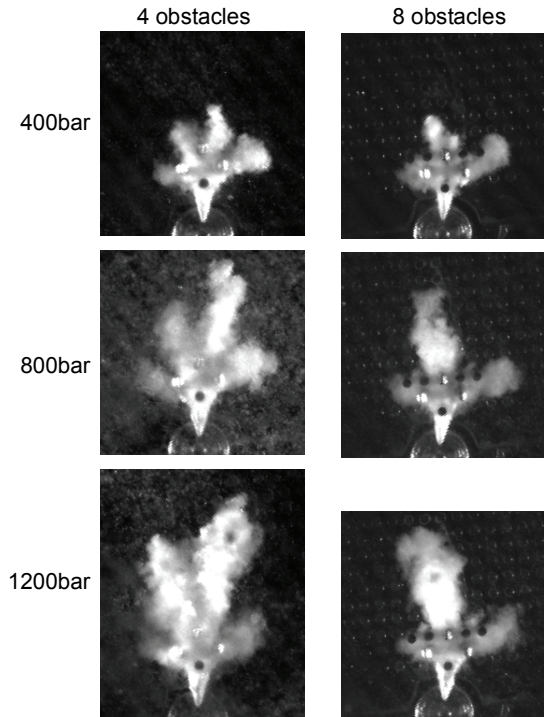


Figure 17: Jet impingement on four- and eight-cylindrical obstacles for three different injection pressures at $t=1200\mu s$ after impingement on the first obstacle

This figure also explains why the middle jet is more compact for 8-obstacles configuration than for 4-obstacles case (see Table 4).

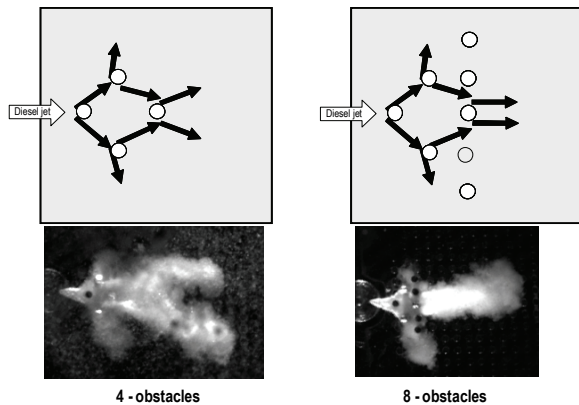


Figure 18: Model comparing jet impingement on four and eight cylindrical obstacles

This similarity is also clearly given analysing the jet length, width and surface area for both geometrical configurations.

Table 4: Distribution angle β_2 by impingement on 4- and 8- obstacles

Configuration	Angle β_2 [°]
4d1, 400 bar	34,8
4d1, 800 bar	34,8
4d1, 1200 bar	31
8d1, 400 bar	16,6
8d1, 800 bar	18
8d1, 1200 bar	16,6

The jet length by impingement on 4- and 8-obstacles for three investigated injection pressures is compared in Fig.19. As indicated in this figure the jet length after impingement on 4-obstacles is practically the same like after impingement on 8-obstacles, independently of injection pressure.

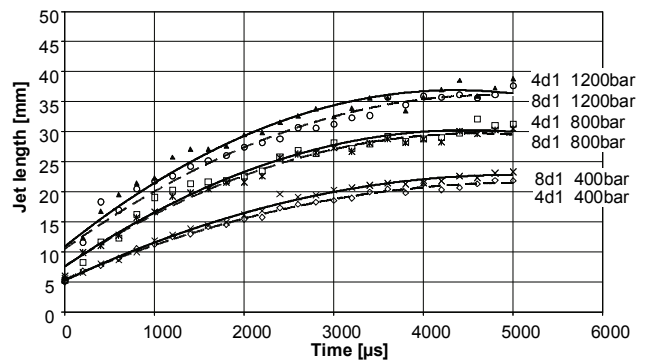


Figure 19: Jet length after impingement on 4- and 8-cylindrical obstacles as a function of time for three different injection pressures (configuration 4d1, 4d2 and 8d1, 8d2)

Almost no effect of number of obstacles or injection pressure is indicated by jet width, as shown in Fig.20. It must be noted that the effect of number obstacles concern small cylinders in the third row.

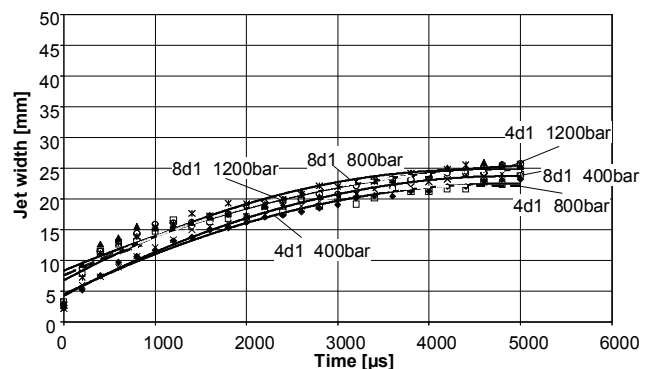


Figure 20: Jet width after impingement on 4- and 8-cylindrical obstacles as a function of time for three different injection pressures (configuration 4d1, 4d2 and 8d1, 8d2)

Also surface area is similar for both investigated configurations, and practically depend only on the injection pressure (Fig.21). Exception is much higher surface area for configuration with 4-obstacles for injection pressure 1200bar. This can be explained by impingement on the obstacles in the third row. Why this effect is observed only for 1200bar is not clear.

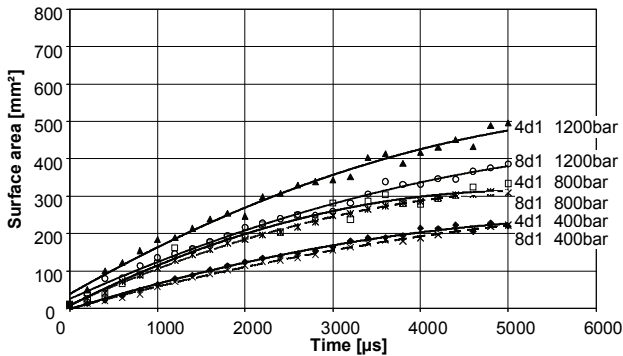


Figure 21: Jet surface area after impingement on 4- and 8-cylindrical obstacles as a function of time for three different injection pressures (configuration 4d1, 4d2 and 8d1, 8d2) (bottom view)

Similarity and differences of Diesel jet impingement on a number of obstacles are indicated in Figure 22. This figure shows jet impingement on multiple obstacles (from four to eight) for injection pressure ($\tau=1500\mu s$) 800bar at two times after impingement: 1200µs and 2000µs.

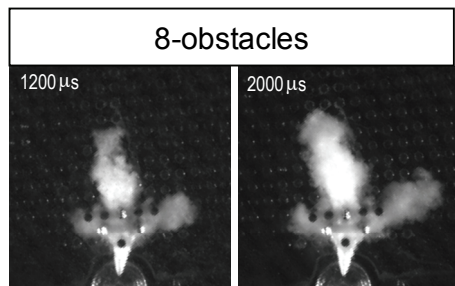
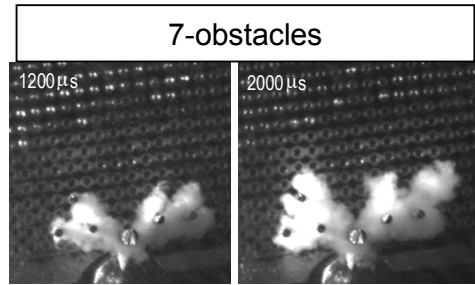
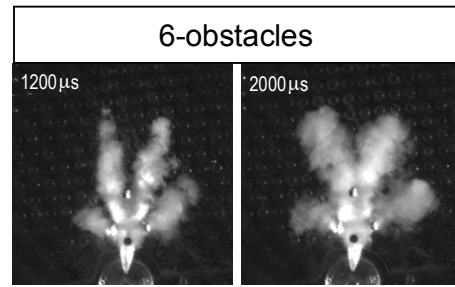
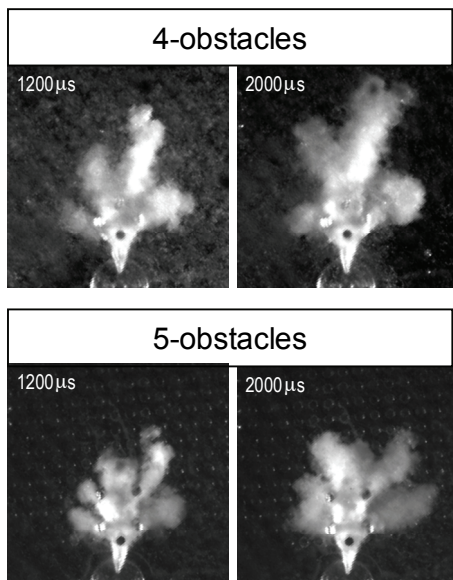


Figure 22: Jet impingement on multiple obstacles (from four to eight) for injection pressure 800bar at two times after impingement: 1200µs and 2000µs ($\tau=1500\mu s$)

Analysis of such experimental data allows creation of phenomenological model for a given configuration giving very good qualitative and even quantitative agreement with experimental data, as shown in Fig.23 for 800bar.

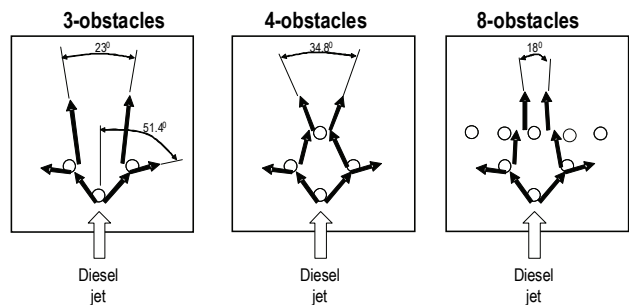


Figure 23: Phenomenological model of Diesel jet impingement on three-four- and eight-cylindrical obstacles for 800bar injection pressure

Phenomenological model for configuration 5d1 and data presented in Figure 23 indicate possibility of very intensive fuel distribution in a selected area

(e.g. combustion chamber) applying Diesel jet impingement on 5-cylindrical obstacles.

A view of the Diesel jet impingement on the five obstacles (configuration 5d1) is given in Figure 24. Contrary to above presented configurations with 3-4- and 8-obstacles, in this case the fuel is pretty well distributed across selected area. Six individual jets may be selected for this configuration.

slightly dependent on the injection pressure. The jet width is mostly dependent on the angle β_1 which increases with increasing injection pressure.

Till now the data presented in this paper were obtained in oil as a surrounding fluid. Additional experiments have also been performed in air at atmospheric pressure.

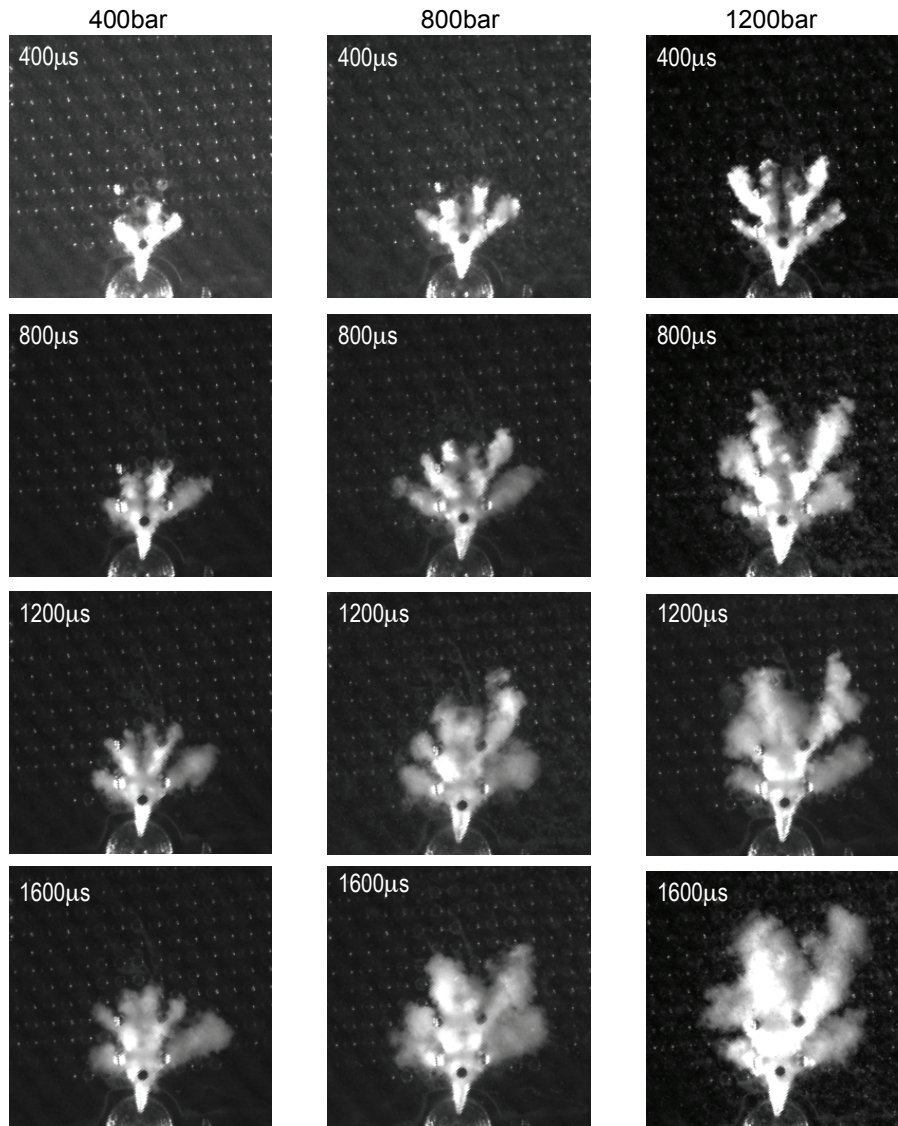


Figure 24: View of Diesel jet impingement on 5-obstacles for three investigated injection pressures as a function of time after jet impingement on the first cylinder

As already observed by other configurations, the jet length after impingement depends on the injection pressure and increases with increasing rail pressure. Much lower dependence on the injection pressure was observed for jet width. Short after impingement on the first obstacle the jet width is still

A view of impingement process from three different angles is shown in Figure 25 at 400µs after impingement on the first obstacles for 8-obstacle configuration and 400bar injection pressure.

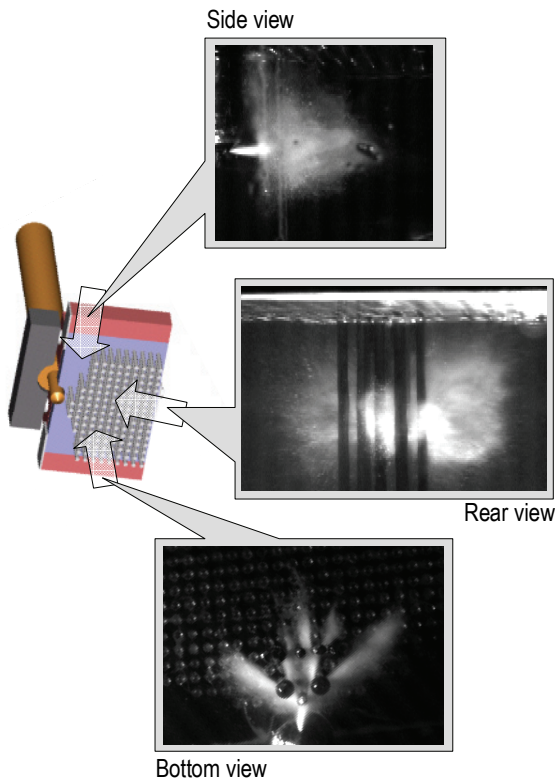


Figure 25: View of impingement process from three different angles at 400µs after impingement on the first obstacles for 8-obstacle configuration and 400bar injection pressure (in air)

Comparison of jet impingement on to 3- and 8-obstacles in air as a surrounding fluid at 400µs after jet impingement on first obstacle is shown in Figure 26. The quality of the process is quite similar to hat observed in oil. Some comparisons between quantitative data obtained in oil and air are discussed below.

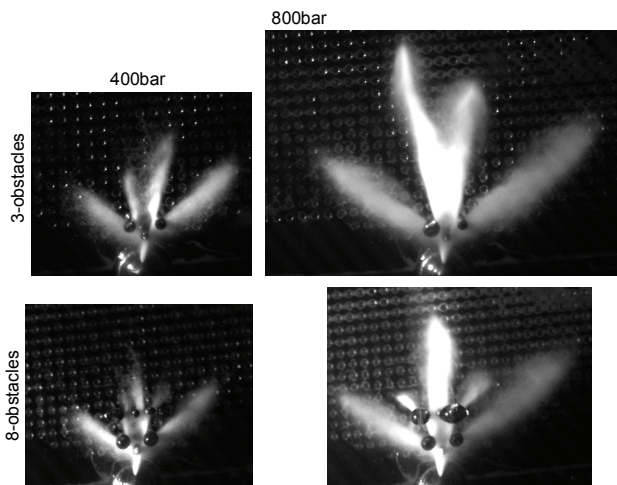


Figure 26: View of jet impingement on to 3- and 8-obstacles in air as a surrounding fluid at 400µs after jet impingement on first obstacle

Figure 27 presents the jet length measured in both surrounding fluids by Diesel jet impingement on cylindrical obstacles for 800bar injection pressure. The jet width is presented in Figure 28.

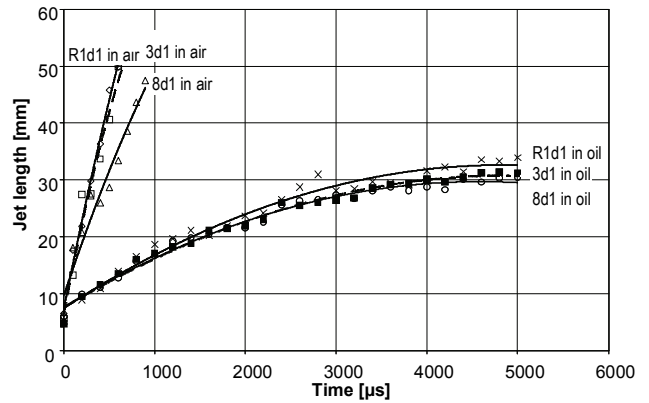


Figure 27: Jet length after impingement on cylindrical obstacles in both surrounding fluids for different geometrical configurations for injection pressure 800bar (bottom view)

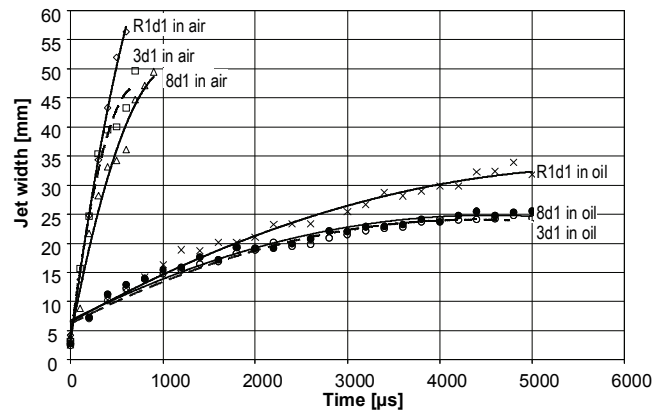


Figure 28: Jet width after impingement on cylindrical obstacles in both surrounding fluids for different geometrical configurations for injection pressure 800bar (bottom view)

6. Concluding remarks

Basic aspects of a high velocity Diesel jet interaction with small cylindrical obstacles are presented in the paper. Especially the effect of high velocity Diesel jet “destruction” and its distribution in space are discussed in the paper. This permits very quick jet distribution in the volume. The dominant role in this process plays a fist obstacle: its diameter, distance from the nozzle outlet and injection pressure play a dominant role in characterization of the jet distribution in space. The jet spatial distribution bases on a multi-jet model.

By Diesel jet impingement on a single obstacle with smaller diameter the distribution angle decreases with increasing injection pressure. For bigger obstacle the angle separating both jets increases being

almost independent of the injection pressure. This angle does not change with time after impingement process, however decreases with increasing distance between nozzle and the obstacle.

For Diesel jet impingement on more than single obstacle, the jet distribution depends on the obstacle geometrical configuration but not necessarily on the number of obstacles. As shown in the paper quite similar distribution has been obtained for three and eight obstacles configurations. Presented phenomenological model explains this observation. Still the geometry of the jets after impinging on the first obstacle defines the distribution on other cylinders. There is possible to design such configuration of small obstacles which permit very good charge homogenization in defined space (combustion chamber). Multi-jet structure permits also higher air entrainment comparing to free jet configuration. All these effects promote fast spatial distribution of Diesel jet, and under hot conditions faster vaporization and better mixing with air.

Acknowledgement

The author thanks Mr. Faltermeier who contributed to performing of experimental investigations.

References

- [1] Bai, C., Gosman, A.D. 1995, Development of Methodology for Spray Impingement Simulation, SAE Technical Paper No. 950283.
- [2] Grover, O.R., Jr., Assanis, D.N. 2001, A Spray Wall Impingement Model Based upon Conservation Principles, The Fifth International Symposium on Diagnostics and Modeling of Combustion in Internal Combustion Engines (COMODIA 2001), July 1-4, 2001, Nagoya.
- [3] Lee, S. and Ryou, H., 2000, Modeling of Spray-Wall Interactions Considering Liquid Film Formation., Proceedings of the Eighth International Conference on Liquid Atomization and Spray Systems, Pasadena, CA, pp. 586-593.
- [4] Mundo, C., Sommerfeld, M., and Tropea, C., 1995, Droplet-Wall Collisions: Experimental Studies of the Deformation and Breakup Process., Int. J. Multiphase Flow 21, pp.151-173.
- [5] Senda, J., Kobayashi, M., Iwashita, S., and Fujimoto, H. 1994, Modeling of Diesel Spray Impingement on a Flat Plate., SAE Technical Paper No. 941894.
- [6] Senda, J., Fujimoto, H., Kobayashi, M., Yamamoto, K., Enomoto, Y. 1995, Heat Transfer Characteristics of a Diesel Spray Impinging on a Wall, Translated from Journal of MESJ, Vo1.29, No.10.
- [7] Weclas, M., Faltermeier, R. 2007, Diesel jet impingement on small cylindrical obstacles formixture

homogenization by late injection strategy, Int. Journal of Engine Research, vol.8, Nr.5, pp.399-413.

[8] Weclas, M. 2006, High velocity CR Diesel jet impingement on to porous structure and its utilization for mixture homogenization in I.C. engines, DITICE Workshop: Drop/wall interaction: Industrial applications, Experiments and Modeling, May, 19th, Bergamo, Italy.

[9] Weclas, M. 2008, Some fundamental observations on the Diesel jet "destruction" and spatial distribution in highly porous structures, Submitted for publication in Journal of Porous Media, vol. 11, No.2, pp.125-145.

[10] Weclas, M., 2005, Porous media in internal combustion engines, [in:] Cellular Ceramics-Structure, Manufacturing, Properties and Applications, Scheffler, M., Colombo, P. (eds), Wiley-VCH-Publ.